Physics and Chemistry of the Earth 144 (2026) 104608

Contents lists available at ScienceDirect

Physics and Chemistry of the Earth

journal homepage: www.elsevier.com/locate/pce

Analysis of channel stability: Evidence from the Middle Brahmaputra floodplains of Assam, India

Nirsobha Bhuyan [a], Haroon Sajjad [a,*], Aastha Sharma [a], Yatendra Sharma [a], Raihan Ahmed [b]

[a] Department of Geography, Faculty of Sciences, Jamia Millia Islamia, New Delhi, India
[b] Department of Geography, Nowgong College, Nagaon, Assam, India

ARTICLE INFO

Keywords:
Channel stability
Riverbank erosion
Channel stability index
River management
Middle Brahmaputra floodplains

ABSTRACT

The middle course of the Brahmaputra River reveals a dynamic behaviour with varying channel planform. The present study aims to assess channel stability using a channel stability index. The river was sectioned into five zones from upstream towards downstream (Z1, Z2, Z3, Z4 and Z5) for a detailed analysis of channel stability from 1990 to 2020 on a decadal basis. The channel stability index was constructed by integrating the parameters of channel activity, average channel width, braiding index and standard sinuosity index for channel stability analysis. The results revealed that Z3 was the most stable reach while Z4 and Z5 exhibited moderate stability. Z1 and Z2 represented the least stable zones. Braiding index, average channel width and channel activity were the key parameters that affected channel stability. The channel was found to be braided and sinuous along its entire course. The effect of topography was more pronounced than channel hydraulics on sinuosity. Easily erodible bank materials, high discharge, substantial sediment load and a gentle channel gradient that reduced stream power contributed to changes in the channel's configuration. Dredging, sediment traps, afforestation and the construction of embankments and porcupines are some suggested measures that could help reduce the risks of channel instability and bank erosion. The study calls for further development and implementation of effective strategies and policies focused on the management of this crucial riverine system.

1. Introduction

Alluvial rivers are characterized by significant variations in their channel morphology and geometry being notably responsive to factors namely discharge, sediment load and tectonic activities (Leopold et al., 1964; Thomas et al., 2019). Modifications in channel morphology and geometry, arising due to bank erosion and accretion, constitute a crucial mechanism of channel adjustment (Simon et al., 2000). Riverbank erosion as a hydro-geomorphological hazard has shaped fluvial ecosystems and also posed substantial environmental and socio-economic challenges for ages (Das et al., 2014). The morphological structure exhibited by rivers in the present times is the consequence of constantly ongoing fluvial processes over many years (Khan et al., 2018). River systems demonstrate dynamic characteristics and strive to achieve equilibrium. This balance is attained through the erosion-accretion processes (Das et al., 2020; Debnath et al., 2017; Hekal, 2018). Erosion and deposition along banks and the resultant bank line shifting occur naturally and constantly (Das and Samanta, 2023) Banks start eroding when the force exerted by the flow of the river exceeds the resistance capacity of the bank materials (Bhattacharya et al., 2022; Konsoer et al., 2016). Bank failure is generally initiated by the removal of the bank's basal sediments due to hydraulic pressure (Ghosh and Sahu, 2019). Apart from hydraulic forces, geotechnical instabilities also significantly contribute to bank collapse. Most failures are caused by a combination of both hydraulic and geotechnical forces (Fischenich, 1989). Rivers typically cause vertical erosion in their upper course by excessively cutting the valley floors whereas lateral erosion is more pronounced in the mid-stretch of the channel (Das et al., 2014; Yousefi et al., 2021). Soft alluvial soil, huge run-off, incessant rainfall, flood discharge, stream power, high sediment load, seismic activities and deforestation accelerate bank erosion (Biswas and Anwaruzzaman, 2019; Debnath et al., 2017; Khan, 2012). Anthropogenic actions namely construction of bridges, barrages and dams have also affected the rate of erosion (Das et al., 2014; Debnath et al., 2023).

Channel planform is closely associated with the erosion and deposition processes (McMahon and Davies, 2018). Bank erosion leads to the

* Corresponding author.
E-mail addresses: nirsobhabhuyan08@gmail.com (N. Bhuyan), haroon.geog@gmail.com (H. Sajjad), aasthasharma389@gmail.com (A. Sharma), syaten25@gmail.com (Y. Sharma), raihan.geog@gmail.com (R. Ahmed).

https://doi.org/10.1016/j.pce.2026.104608
Received 17 August 2024; Received in revised form 11 June 2026; Accepted 17 June 2026
Available online 17 June 2026

shifting of bank lines and induces various alterations along the banks and within the channel itself (Ahammed and Pandey, 2019; Chakraborty and Saha, 2022; Sarma et al., 2007). In alluvial plains, rivers usually assume three primary patterns namely braided, meandering and straight (Leopold and Wolman, 1957). When the rivers reach their maximum sediment carrying capacity, meandering single-channels may transform into braided streams through sediment deposition on the riverbed (Das et al., 2014; Siddha and Sahu, 2022). Lateral erosion is primarily evident in floodplains characterized by a low-lying terrain of readily erodible materials primarily due to a larger sediment load and a gentler gradient that slows down the velocity of rivers (Dey and Mandal, 2019). Consequently, the rivers wear away their channel walls leading to the accumulation of more silt. The sediment deposited on the riverbed forms sandbars and constricts the channels, thereby intensifying erosion (Ahmed et al., 2018). These gradual processes ultimately result in the shifting of the channels over time. The floodplains attract millions of inhabitants due to their favourable topography and the presence of fertile soils favourable to agriculture. Despite supporting a rich biodiversity and various ecosystems, floodplains are highly susceptible to riparian erosion (Acharjee, 2022; Hazarika et al., 2015).

Channel stability is influenced by forms, patterns and dimensions of channels and erosion-accretion processes (Haron et al., 2022). Channel stability and planform changes have been observed by various scholars in different regions globally. Thomas et al. (2019) assessed channel stability in the lower stretches of the Krishna River during 1973-2015 through erosion-deposition activities and braiding. Soar et al. (2017) quantified channel stability using a river energy audit scheme (REAS). Yang et al. (2023) and Yu and Xu (2023) studied channel stability in the Chinese rivers of Songhua and Huaihe respectively. Channel width, channel activity, braid index and net channel change were used by Nelson et al. (2013) to analyze channel changes in the Snake River, Wyoming. Sah and Das (2018) identified the morphological changes that occurred due to erosional activities in the Brahmaputra plains. A study based on the morphodynamics was carried out by Hosu and Sabo (2012) on the Somes River in Northwestern Romania. Channel planform was also examined by Jodhani et al. (2024), Ghosh and Mukhopadhyay (2021), Deb and Ferreira (2015) and Mandarino et al. (2019) in the Rel River (Western India), Dwarkeswar River (Eastern India), Manu River (Bangladesh) and Scrivia River (Italy) respectively. Channel planform was studied using the sinuosity index by Khan et al. (2018) and Ratzlaff (1991) in the Yamuna floodplain, India and the Upper Saline River Valley, Western Kansas respectively. Morphological changes were also analyzed by Nath and Ghosh (2022) using the sinuosity index and prediction of river discharge in the Barak River of Assam, India.

The Brahmaputra River manifests profound morphological changes. The physical setting of the Himalayas impacts the river's fluvial regime resulting in irregular flow behaviour, channel alignment, meander expansion and avulsion (Kotoky et al., 2015). The river while entering the plains of Assam, flows through an alluvial valley and causes severe bank erosion. Nearly the entire river displays a multi-channel nature with most sections featuring three to six channels divided by islands and bars during low flood. As the water level rises, the islands and mid-channel bars get either submerged or vanish completely. The arrangement of channels undergoes frequent alterations leading to extensive erosion in the floodplains and the formation of sandbars (Northwest Hydraulics Consultants, 2006). Sharma et al. (2010) found that the Brahmaputra eroded a total of 538.805 km^2 on its right bank and 914.62 km^2 on its left bank between 1990 and 2007-08. Saikia et al. (2019) estimated that from 1973 to 2014, the total area eroded by the river was 1557 km^2 of which the left and right banks recorded 829 km^2 and 728 km^2 of land loss respectively. Gilfellon et al. (2003) noted inconsistencies in channel shifting, braiding and bed profile of the Brahmaputra over time and space. Akhtar et al. (2011) correlated the river's braiding with stream power and concluded that channel braiding increased with a decrease in stream power which has the potential to accelerate bank erosion. A study by Sarma and Acharjee (2018) recorded variable braiding in the Brahmaputra and established a positive correlation between braiding and channel width. Suresh et al. (2022) evaluated the sinuosity for a stretch of the Brahmaputra in Upper Assam which suggested a shift in the river's course between 1990 and 2021 wherein the river migrated southward. Sahay et al. (2020) calculated the braiding and sinuosity indices for the Brahmaputra along Majuli Island. Sarma et al. (2007) and Gogoi and Sharma (2021) also conducted studies on the morphodynamics of the Brahmaputra and presented intricate hydrogeological details of the river and its basin.

The Brahmaputra is morphologically a very active river and its dynamics might change within a relatively shorter duration. The Middle Brahmaputra floodplains experienced a loss of more than 300 km^2 of land between 1990 and 2020 and have been recognized as significantly vulnerable to bank erosion (Bhuyan et al., 2023, 2024). Hence, analyzing the Middle Brahmaputra River's channel stability and the nature of bank erosion is imperative. Studies on river morphodynamics have been carried out earlier on the Brahmaputra and other rivers worldwide, however, most studies focused on individual parameters. Research based on multiple planform parameters is notably scant in the existing literature. This paper, therefore, aimed to assess the channel stability in the Middle Brahmaputra River using a channel stability index derived through different planform parameters namely channel activity, average channel width, braiding index and standard sinuosity index. The index-based approach of the study also helped to identify the priority zones to put effort in the areas that need urgent attention for minimizing the risks posed by channel instability. The methodological framework used in this study could be applied across different spatial units for channel stability analysis. This piece of research provides a holistic view of erosion-deposition and channel stability scenarios in the Middle Brahmaputra River and its floodplains for devising and implementing river and floodplain management strategies.

2. Study area

The Middle Brahmaputra floodplains in Assam span an area of 7294.85 km^2, extending from 26°11′3″ N to 26°58′24″ N latitudes and 91°52′14″ E and 93°53′16″ E longitudes (Fig. 1). The Brahmaputra, a significant trans-Himalayan river originating in southern Tibet, traverses across the study area for roughly 250 km. The river manifests a braided pattern in the Assam plains which is a consequence of a gentle gradient of the riverbed and high sediment loads. The deposition of the sediments leads to the formation of numerous sandbars, locally referred to as chars and chaporis, amidst multiple distributary channels. The major tributaries include the Jia Bharali which joins the Brahmaputra on its right bank and the Kolong, Kopili and Dhansiri that merge with the Brahmaputra on the left bank.

The floodplains encompass six districts namely Morigaon, Darrang, Nagaon, Sonitpur, Golaghat, and Biswanath with a population exceeding three million (Census of India, 2011). Predominant soil types in the study area include alluvial and red loamy soils. Parts of the floodplains lie over a bed of hard crystalline rocks dating back to the pre-Cambrian era (Kumar et al., 2020; Rajmohan and Prathapar, 2013). The climate is characterized by high humidity and an average annual rainfall of 2500 mm. Mild summers and winters prevail with the minimum and maximum temperatures around 16°C and 39°C respectively. The floodplains host a diverse range of habitats and biodiversity with prominent tree species like sal, *Terminalia*, *Ficus*, and *Lagerstroemia*. Animal species such as the royal Bengal tigers, one-horned rhinoceros, spotted deer and swamp buffaloes thrive in this habitat alongside numerous birds, insects and aquatic life. National parks namely Kaziranga and Orang and the wildlife sanctuaries of Laokhowa and Pobitora are located in the study area. Wetlands, locally called beel, are also integral to the floodplains. Despite offering opportunities for hydropower, irrigation, recreation, navigation and pisciculture, the study area grapples with multiple challenges. Riverbank erosion and floods pose serious threats to the region, exacerbated by its location in the tectonically

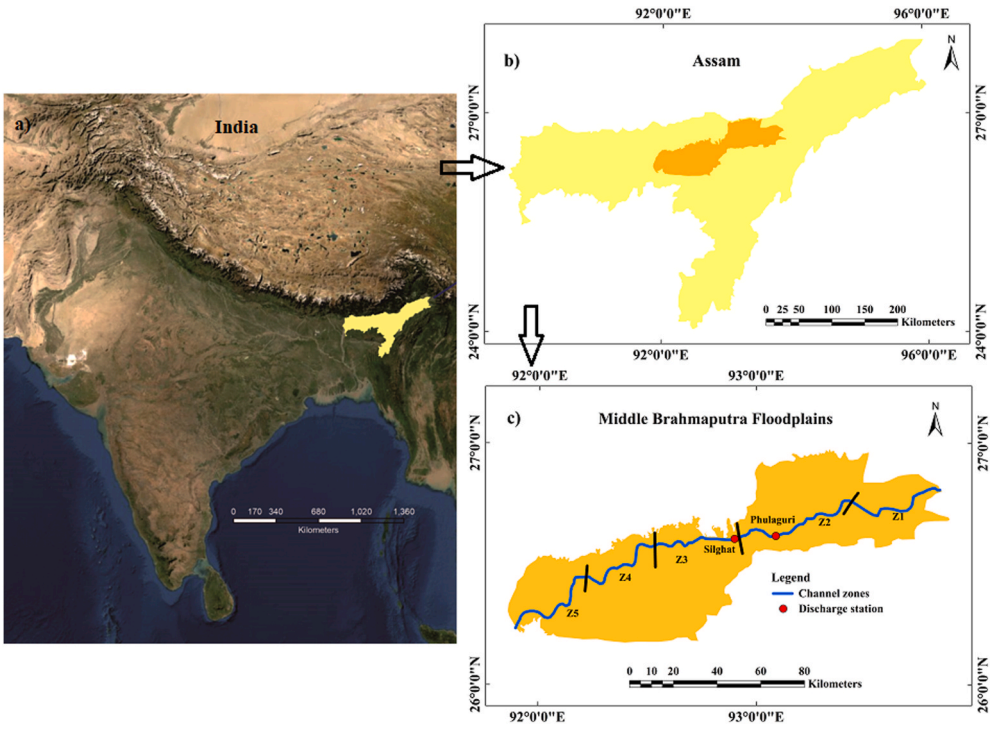

Fig. 1. a) Location of Assam within India b) Middle Brahmaputra floodplains in Assam c) Channel zones in the floodplains.

fragile seismic zone V. The Brahmaputra's reputation as 'the sorrow of Assam' reflects the severity of its impacts including severe floods and bank line oscillations which necessitates concerted efforts for mitigation and management of the floodplains.

3. Methodology

The present study involved the use of satellite imageries to extract the river channels and estimate the channel stability parameters of channel activity, average channel width, braiding index and standard sinuosity index. These parameters were further employed to construct a channel stability index to assess channel stability. The study was executed on a decadal basis from 1990 to 2020. The detailed methodological framework is presented in Fig. 2.

3.1. Extraction of river channels and delineation of channel zones

The satellite imageries for delineating the river channels were obtained from the United States Geological Survey (USGS) Earth Explorer for the years 1990, 2000, 2010 and 2020. Landsat 4/5 imageries were

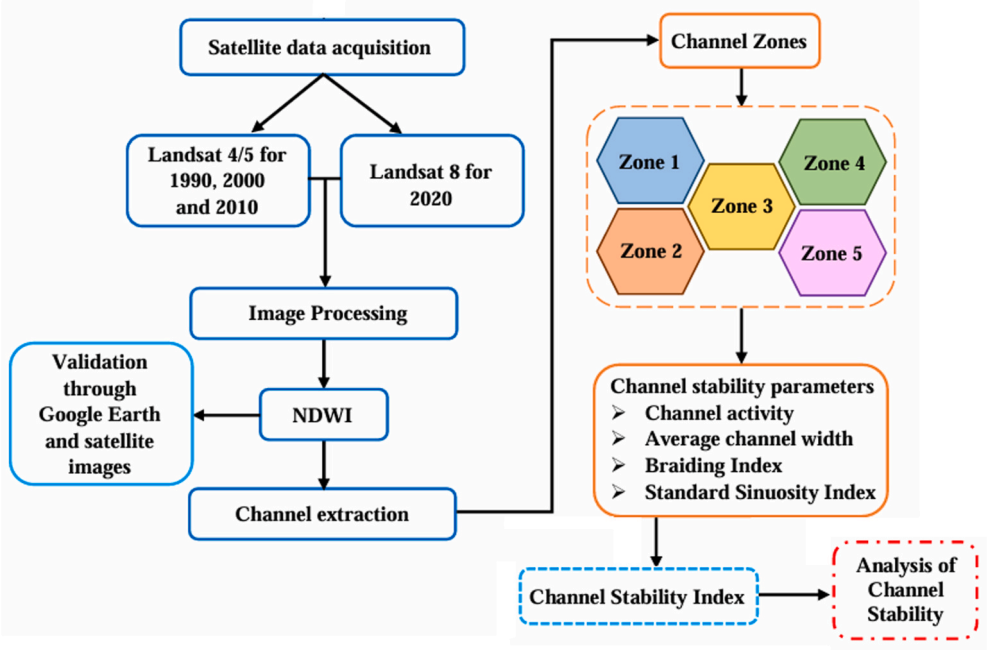

Fig. 2. Methodological framework for the study.

utilized for 1990, 2000, and 2010 while Landsat 8 imageries were employed for 2020. Post-monsoon imageries with low or absence of cloud cover were used for legible identification of river channels. The images were processed in ArcGIS 10.8 software through layer stacking, rectification, enhancement, mosaicking and masking. The normalized difference water index (NDWI) was determined for distinct channel extraction. Subsequently, the NDWI images were reclassified into 'waterbody' and 'non-waterbody' classes, providing a clear distinction between river channels and other land cover. The reclassified images were validated by comparing those with the original satellite imageries and Google Earth Pro to ensure accuracy. The river channels were then digitized from the NDWI images in the form of polygons. Sarkar et al. (2012) also utilized NDWI images for effective and accurate channel extraction. The extracted channels were sectioned into five zones namely Z1, Z2, Z3, Z4 and Z5 based on equal distance from upstream to downstream (Fig. 1c).

3.2. Estimation of channel stability parameters

A channel attains stability when it maintains its pattern, dimension and rates of erosion-deposition (Endreny, 2006). The primary forms of channel instability include channel form adjustments, meandering and bank erosion (Zesmill, 2016). Thus, factors like channel activity, average channel width, braiding and sinuosity reflect the degree of channel stability. If higher fluctuations are recorded for these parameters over a period of time, the channel represents higher instability.

3.2.1. Channel activity

Channel activity refers to the total area encompassing both erosion and accretion occurring within the river channel per year per unit longitudinal distance (Kuo et al., 2017; Nelson et al., 2013; Wu et al., 2023). Thus, areas of erosion and deposition were calculated to estimate channel activity. The areas of erosion and accretion were obtained through overlay analysis for three decades (1990-2000, 2000-2010 and 2010-2020). The extracted river channels for two consecutive years were overlaid and the unchanged area of the river channel was calculated using the intersect tool. Further, the erase tool was used to estimate the areas of erosion and accretion. The unchanged area was erased from a decade's latest year to derive the eroded area. Similarly, the unchanged area was erased from the base year of the decade to determine the accreted area. Channel activity was calculated as:

$$CA = (Eroded\ area + Accreted\ area) / (CL_1) / (Y_2 - Y_1) \quad (1)$$

where CA is channel activity, CL_1 is the channel length based on the channel's centre line of the base year, Y_1 is the base year and Y_2 is the latest year.

3.2.2. Average channel width

The average channel width was determined for each zone year-wise by measuring the perpendicular distance between the two banks (right bank and left bank) at an interval of 10 km using the measure tool. After the widths were measured, the mean was calculated for every zone of each year to derive the average widths.

3.2.3. Braiding index

Braiding index shows the interweaving nature of a river channel which reflects its sediment transport ability. This was computed as the ratio of the total channel length (summation of the primary channel length and all secondary channels' length) to the primary channel length on the basis of the channel's centreline. If the braiding index is greater than 1.5, the river qualifies as a braided river (Sarma and Acharjee, 2018). It is calculated as:

$$BI = \frac{CL + SCL}{CL} \quad (2)$$

where BI is braiding index, CL refers to the channel length (primary channel) and SCL denotes the length of all secondary channels.

3.2.4. Sinuosity index

Sinuosity index provides a measure of the channel pattern of a river system and determines if the channel is straight, sinuous or meandering (Mueller, 1968). Straight streams have a sinuosity index value of 1 while meandering streams usually exhibit a value of 1.5 or more (Leopold and Wolman, 1957; Ratzlaff, 1991). Standard sinuosity index is calculated as:

$$SSI = \frac{CL}{VL} \quad (3)$$

where SSI represents standard sinuosity index, CL denotes the channel length and VL refers to the valley length. Valley length is the distance along a line equidistant from the bases of both the valley walls (Mueller, 1968). In this case, the left and right banks are considered the valley walls. It is determined as:

$$VL = \frac{AA' + BB'}{2} \quad (4)$$

where AA' and BB' are the length of the left and right banks of each zone of the channel respectively. The valley length was computed in ArcGIS through digitization and calculate geometry tool. The numeric data was then extracted from the attribute table for relevant analysis. A similar methodology was also adopted by Ghosh and Mistri (2012) and Khan et al. (2018).

Though SSI is an excellent channel planform index, it fails to explain whether the pattern assumed by the channel has been influenced by hydraulic, topographic or both factors (Mueller, 1968). Therefore, hydraulic and topographic sinuosity indices were estimated to overcome this drawback. The combined value of the hydraulic and the topographic sinuosity indices is always equal to 100. As a result, only a single index needs to be computed since the other value can be derived by subtracting the calculated value from 100. For instance, if the hydraulic sinuosity index is determined to be 50, it signifies that half of the river's sinuosity is attributed to hydraulic factors while the remaining half is inherently associated with topographic influences. In addition, channel index and valley index were also determined to aid the calculation of hydraulic and topographic sinuosity indices:

$$CI = \frac{CL}{SL} \quad (5)$$

$$VI = \frac{VL}{SL} \quad (6)$$

$$HSI = \%\ equivalent\ of\ \frac{CI - VI}{CI - 1} \quad (7)$$

$$TSI = \%\ equivalent\ of\ \frac{VI - 1}{CI - 1} \quad (8)$$

where CI is the channel index, VI denotes valley index, CL indicates the channel length, SL is the straight length denoting the shortest distance between the start and end points of a channel, HSI refers to hydraulic sinuosity index and TSI represents topographic sinuosity index. Straight length was also calculated using a similar approach as that of valley length through digitization. The geometry was then calculated in the attribute table.

3.3. Calculation of channel stability index

A channel stability index (CSI) was constructed following Kuo et al. (2017) to assess channel stability using the parameters of channel activity, average channel width, braiding index and sinuosity index. The

values of these parameters were averaged year-wise for every zone. Subsequently, the standard deviation and the coefficient of variance (CV) were computed for every parameter. A higher CV indicates a greater dispersion from the mean, suggesting instability in a zone. The CVs of the four parameters were then added for each zone to derive the CSI:

$$CV_{CA} + CV_{ACW} + CV_{BI} + CV_{SSI} = CSI \quad (9)$$

The channel stability scores were grouped into three categories of high, moderate and low. A higher CSI implies higher channel instability and vice-versa. The grading thresholds were defined using natural breaks which reduced intra-class variance and enhanced inter-class variance. This method provides a practical framework for evaluation and assists in channel regulation practices (Kuo et al., 2017).

4. Results

The morphological nature of a river depends upon various attributes associated with channel planform. Such numeric information of the channel aids in the calculation of the planform indices which further help in stability assessment. These characteristics of the river channel zones have been mentioned in Table 1.

4.1. Evaluation of erosion, deposition and channel activity

Significant variations were observed in the erosion-accretion activities in the river channel. Of all zones, Z2 experienced the highest erosion (77.47 km^2) during 1990-2000 and the highest deposition (80.69 km^2) during 2000-2010 (Table 2, Fig. 3). However, the highest net area change was noticed in Z3 between 1990 and 2000 which accounted for 37.48 km^2 of land gain. Z3 also encountered the highest negative net area change of 10.31 km^2. A positive net change corresponds to an overall gain of land whereas a negative net change indicates an overall loss of land. Deposition was more than erosion across all zones during 1990-2000 except Z2. A similar situation was observed between 2000 and 2010 where deposition surpassed erosion in all zones apart from Z5. Hence, Z1, Z3, Z4 and Z5 and Z1, Z2, Z3 and Z4 noted a negative net area change during 1990-2000 and 2000-2010 respectively. On the other hand, Z2 and Z5 underwent positive net area changes during the same period. However, in the last decade of 2010-2020, a reverse condition was noticed where erosion exceeded accretion across all zones. Therefore, all zones faced a negative net area change. Channel activity which is based on the area of erosion and accretion, was observed to be the highest in Z4 during 1990-2000. Conversely, the lowest channel activity was seen in Zone 1 between 2010 and 2020.

4.2. Analysis of average channel width

The average channel width varied spatially and temporally. The channel was the widest in Z1 (11.23 km) followed by Z4 (11 km) in the year 2000 (Table 3). On the other hand, the narrowest stretches were identified in Z2 (5.60 km) followed by Z5 (5.89 km) in 2020. Z1, Z3 and Z4 experienced an increase in the average channel width from 1990 to 2000 whereas the average channel width decreased for Z2 and Z5 during this period (Table 4). In the second decade of 2000-2010, apart from Z2, all other zones encountered a decrease in the average channel width. In the last decade of 2010-2020, there was a reduction in the average channel width for all the zones.

4.3. Analysis of braiding index

The analysis of the BI values has shown that the Middle Brahmaputra River is a braided channel exhibiting values greater than 1.5. The highest braiding was observed in Z1 (BI = 10.41) followed by Z5 (10.02) in 2000 (Table 3). Significant braiding also took place in Z2 and Z4 in 2000 and Z1, Z2 and Z3 in 2010 where the BI was measured over 9. Between 1990 and 2000, all five zones recorded an increase in the BI (Table 4). However, an opposite trend was observed in the next two decades (2000-2010 and 2010-2020) where all the zones experienced a decrease in the BI except Z2 during 2000-2010.

4.4. Analysis of sinuosity index

The SSI values ranged from 1.25 to 1.01 throughout the zones during 1990-2020 (Table 3). This showed that the river is sinuous and close to straight in some zones but it does not qualify as a meandering channel since the SSI values were below 1.5. The SSI registered a decrease in every zone between 1990 and 2000 but demonstrated a fluctuating trend in the next two decades across all zones (Table 4). The differences in the SSI values, however, were not very significant for most zones. The most sinuous stretch was Z1 in 1990 and 2010. Z3 and Z5, Z2, Z3, Z4 and Z5, Z2, Z3, Z4 and Z5 and Z2, Z3 and Z5 in 1990, 2000, 2010 and 2020 respectively were found to be almost straight since the SSI values were close to 1. Therefore, these reaches could possibly transition into straight channels in the future years. However, given the unpredictable nature of the Brahmaputra, a converse situation might also occur wherein the channels in various zones perhaps become more sinuous.

Table 1
Characteristics of the channel zones used for determining parameters of channel stability.

Zones	Years	Channel Length (in km)	Valley Length (in km)	Straight Length (in km)	Channel Index	Valley Index	Secondary Channels' Length (in km)
Z1	1990	51.68	42.32	41.20	1.25	1.03	245.44
	2000	49.94	43.65	39.64	1.26	1.10	469.97
	2010	53.47	42.66	40.01	1.34	1.07	464.98
	2020	50.18	44.13	39.47	1.27	1.12	389.09
Z2	1990	66.91	60.35	53.10	1.26	1.14	248.05
	2000	62.92	61.06	54.42	1.16	1.12	523.44
	2010	62.31	61.94	53.72	1.16	1.15	528.22
	2020	61.24	60.20	53.76	1.14	1.12	356.12
Z3	1990	47.74	46.33	40.58	1.18	1.14	300.86
	2000	48.40	47.75	39.52	1.22	1.21	341.10
	2010	50.52	48.78	40.80	1.24	1.20	313.39
	2020	42.74	42.44	39.19	1.09	1.08	258.14
Z4	1990	41.35	37.84	33.35	1.24	1.13	300.44
	2000	39.53	38.30	33.85	1.17	1.13	335.60
	2010	39.70	39.20	34.35	1.16	1.14	320.82
	2020	44.57	40.22	33.25	1.34	1.21	232.34
Z5	1990	47.85	46.08	39.15	1.22	1.18	257.55
	2000	44.17	42.74	39.06	1.13	1.09	398.29
	2010	47.57	45.75	39.07	1.22	1.17	341.34
	2020	50.33	49.30	38.85	1.30	1.27	247.61

Table 2
Area of erosion-accretion and channel activity.

Zones	Duration	Erosion ($km^{2)}$	Accretion (km^2)	Unchanged (km^2)	Net change (km^2)	Channel Activity (km^2/km/year)
Z1	1990-2000	55.08	65.28	25.18	10.20	0.23
	2000-2010	51.90	64.99	15.26	13.09	0.23
	2010-2020	48.88	47.08	20.08	−1.80	0.18
Z2	1990-2000	77.47	75.53	34.58	−1.94	0.23
	2000-2010	62.79	80.69	31.36	17.90	0.23
	2010-2020	72.93	62.67	31.48	−10.26	0.22
Z3	1990-2000	43.01	80.49	27.73	37.48	0.26
	2000-2010	46.31	48.23	25.51	1.92	0.20
	2010-2020	57.70	47.39	21.43	−10.31	0.21
Z4	1990-2000	47.66	78.08	28.84	30.42	0.30
	2000-2010	51.80	53.32	23.18	1.52	0.27
	2010-2020	60.77	54.87	20.10	−5.90	0.29
Z5	1990-2000	53.61	72.23	32.2	18.62	0.26
	2000-2010	60.87	60.22	25.59	−0.65	0.27
	2010-2020	67.93	59.17	27.28	−8.76	0.27

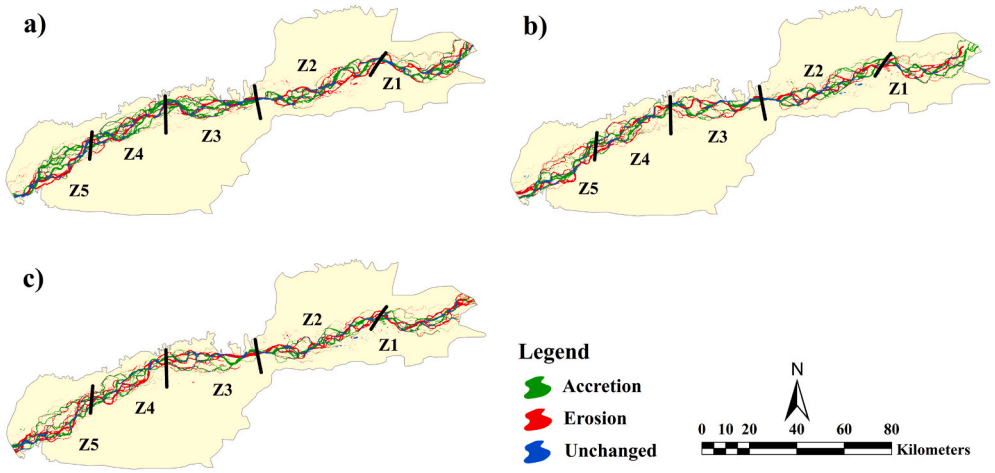

Fig. 3. Decadal erosion-accretion in channel zones during a) 1990-2000 b) 2000-2010 c) 2010- 2020.

Table 3
Values of channel stability parameters.

Zones	Years	Average Channel Width (in km)	Braiding Index	Standard Sinuosity Index
Z1	1990	6.08	5.75	1.22
	2000	11.23	10.41	1.14
	2010	9.88	9.70	1.25
	2020	8.40	8.75	1.14
Z2	1990	8.50	4.71	1.11
	2000	7.80	9.32	1.03
	2010	8.27	9.48	1.01
	2020	5.60	6.82	1.02
Z3	1990	6.33	7.30	1.03
	2000	7.84	8.05	1.01
	2010	7.39	7.20	1.04
	2020	6.22	7.04	1.01
Z4	1990	8.02	8.27	1.09
	2000	11.00	9.49	1.03
	2010	8.20	9.08	1.01
	2020	7.25	6.21	1.11
Z5	1990	6.46	6.38	1.04
	2000	9.46	10.02	1.03
	2010	6.97	8.18	1.04
	2020	5.89	5.92	1.02

HSI and TSI values represented the relative contributions of hydraulic and topographic factors to channel sinuosity. Both hydraulic and topographic factors were found to have contributed to the sinuous nature of the river. The hydraulic factors had the highest impact on Z1 throughout the time period compared to the other zones while the influence of topography was found to vary spatially and temporally (Table 5). The TSI increased for Z1, Z2, Z3 and Z4 and Z2, Z4 and Z5 during 1990-2000 and 2000-2010 respectively. It subsequently increased for three zones (Z1, Z3 and Z5) between 2010 and 2020. On the contrary, only one zone (Z5) experienced an increase in HSI between 1990 and 2000. Z1 and Z3 noted an increase in HSI from 2000 to 2010 whereas Z2 and Z4 experienced an increase during 2010-2020.

4.5. *Assessment of channel stability*

Channel stability was studied using a channel stability index (CSI). It was derived as a function of channel activity, average channel width, braiding index and sinuosity index. The CV values of each parameter for every zone were added to calculate the SI. A higher CSI indicated higher channel instability. The CSI values were classified into three classes namely high (>50%), moderate (40%-50%) and low (<40%). The highest channel stability was exhibited in Z3 (Table 6, Fig. 4). Z4 and Z5 showed moderate channel stability while Z1 and Z2 represented the most unstable reaches. The channel stability was mostly influenced by channel width followed by braiding in Z1 and Z4. In Z2 and Z5, braiding was the dominant factor that controlled channel stability followed by channel width. Channel activity and channel width primarily impacted channel stability in Z3.

5. Discussion

The Middle Brahmaputra River is dynamic in nature owing to its vast and varying channel widths, unstable planform character and

Table 4
Decadal changes in channel stability parameters.

Zones	Duration	Average Channel Width (in km)	Braiding Index	Standard Sinuosity Index
Z1	1990-2000	5.15	4.66	−0.08
	2000-2010	−1.35	−0.71	0.11
	2010-2020	−1.48	−0.95	−0.11
Z2	1990-2000	−0.70	4.61	−0.08
	2000-2010	0.47	0.16	−0.02
	2010-2020	−2.67	−2.66	0.01
Z3	1990-2000	1.51	0.75	−0.02
	2000-2010	−0.45	−0.85	0.03
	2010-2020	−1.17	−0.16	−0.03
Z4	1990-2000	2.98	1.22	−0.06
	2000-2010	−2.80	−0.41	−0.02
	2010-2020	−0.95	−2.87	0.10
Z5	1990-2000	3.00	3.64	−0.01
	2000-2010	−2.49	−1.84	0.01
	2010-2020	−1.08	−2.26	−0.02

Table 5
Values of sinuosity assessment parameters.

Zones	Years	Hydraulic Sinuosity Index	Topographic Sinuosity Index
Z1	1990	88.00	12.00
	2000	46.15	53.85
	2010	22.22	77.78
	2020	45.83	54.17
Z2	1990	18.18	81.82
	2000	61.54	38.46
	2010	25.00	75.00
	2020	4.55	95.45
Z3	1990	23.53	76.47
	2000	30.77	69.23
	2010	79.41	20.59
	2020	6.67	93.33
Z4	1990	16.67	83.33
	2000	12.50	87.50
	2010	22.73	77.27
	2020	55.56	44.44
Z5	1990	14.29	85.71
	2000	11.11	88.89
	2010	38.24	61.76
	2020	10.00	90.00

fluctuating erosion-deposition rates. The primary source of channel instability is sediment load (Rakovan and Renwick, 2011; Tarrio et al., 2024). The Brahmaputra is a perennial river which emerges from the Himalayas and flows through various terrains accumulating large quantities of sediment. In the floodplains, the sedimentary materials consisting of silt and fine sand deposited along the banks are loosely arranged rendering these areas highly prone to erosion (Nath and Medhi, 2021). Following the Assam Earthquake of 1950, erosion and floods became common occurrences in the Brahmaputra valley. The earthquake-induced landslides generated substantial amounts of sediment, contributing to the river's sediment load (Bhuyan et al., 2023). The average sediment load of the Brahmaputra is estimated to be approximately 250 million metric tonnes/year in the eastern part of the river in Assam which increases to almost 500 million metric tonnes/year in the western part (Northwest Hydraulics Consultants, 2006). Such a high sediment load is suggestive of the river's significant channel width, creation of a braiding pattern and severe erosion-accretion. The channel starts depositing the bed sediment load which is composed of coarse sands since the channel is unable to transport it any longer. The deposition of these coarse sediments becomes the core of sand bar formation which gradually develops into an island (Leopold and Wolman, 1957). When the stream hits these bars, it gets bifurcated and diverted toward the banks causing channel widening which accelerates the process of bank erosion (Akhtar et al., 2011). Since numerous bars form within the channel, the river assumes a braiding pattern. Moreover, a low channel gradient reduces the river's velocity and hastens the process of deposition of sediment within the channel (Schumm, 1961; Zischg, 2023). Therefore, a higher sediment load will lead to increased deposition in the channel, consequently leading to a wider channel and increased braiding, hence, channel instability (Mehtani, 2017). Channel instability and the presence of easily erodible soils would further lead to bank erosion.

The most stable reach of the channel was Z3. This zone was found to have a relatively narrow valley width owing to the presence of rocky hills. The area from Silghat to Tezpur represented node points which were composed of Precambrian gneisses (Sarma and Phukan, 2006). Such resistant topography ensured limited channel activity and braiding, a narrower channel and a nearly sinuous channel, thereby leading to channel stability. Z4 and Z5, located downstream of Z3 were moderately stable reaches. Channel activity, average channel width and braiding contributed to instability in these zones. The width of the channel was constricted in the node point of Z3. Consequently, when the river crossed this node point, the channel widened to accommodate the increased water volume. The deposition of sediments occurred after this node point in Z4 and Z5 which caused the channel to become shallower. Therefore, the high sediment load resulted in considerable channel activity, especially deposition within the channel in the form of mid-channel bars. The cumulative deposition in Z4 and Z5 during 1990-2020 was 377.89 km^2. This facilitated an increase in the channel width and braiding. A similar scenario was prevalent in Z1 and Z2 which were highly unstable stretches of the channel. These zones were situated downstream of a node point around Salmora in Majuli. Substantial channel activity was observed in these reaches and deposition accounted

Table 6
Values of channel stability index

Zones	Average Channel Width (in km)			Braiding Index			Standard Sinuosity Index			Channel Activity (km^2/km/year)			Channel Stability Index	Priority Zones
	Mean	SD	CV (%)	Mean	SD	CV (%)	Mean	SD	CV (%)	Mean	SD	CV (%)		
Z1	8.90	1.910	21.47	8.65	1.780	20.53	1.19	0.049	4.10	0.21	0.024	11.22	57.32%	✓
Z2	7.54	1.327	17.60	7.58	2.270	29.93	1.04	0.046	4.39	0.23	0.005	2.05	53.97%	✓
Z3	6.95	0.796	11.46	7.40	0.448	6.05	1.02	0.015	1.47	0.22	0.026	11.93	30.91%	–
Z4	8.62	1.641	19.04	8.26	1.459	17.67	1.06	0.048	4.49	0.29	0.012	4.30	45.50%	✓
Z5	7.20	1.573	21.85	7.63	1.871	24.52	1.03	0.010	0.93	0.27	0.005	1.75	49.05%	✓

SD = Standard deviation, CV = Coefficient of variation.

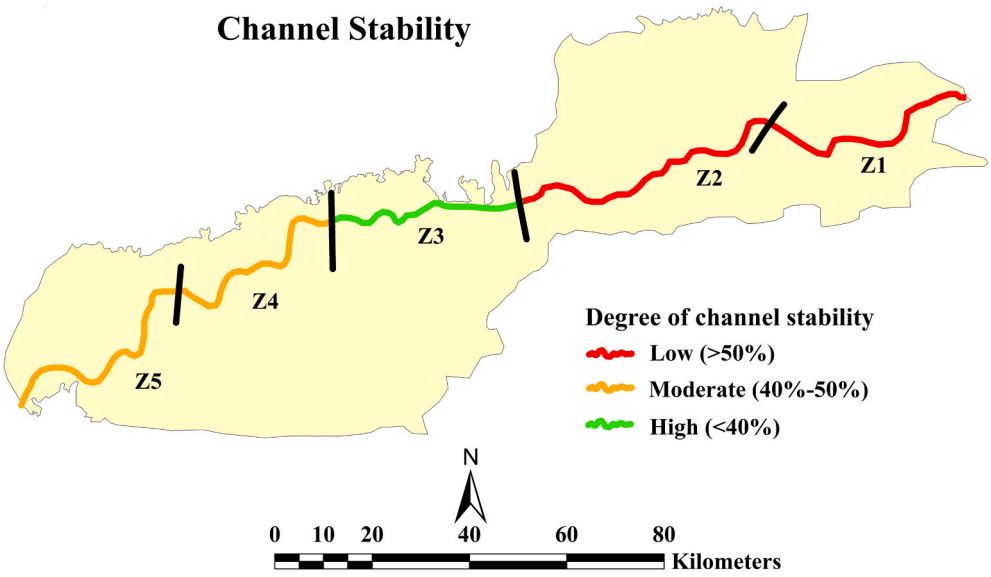

Fig. 4. Channel stability of channel zones.

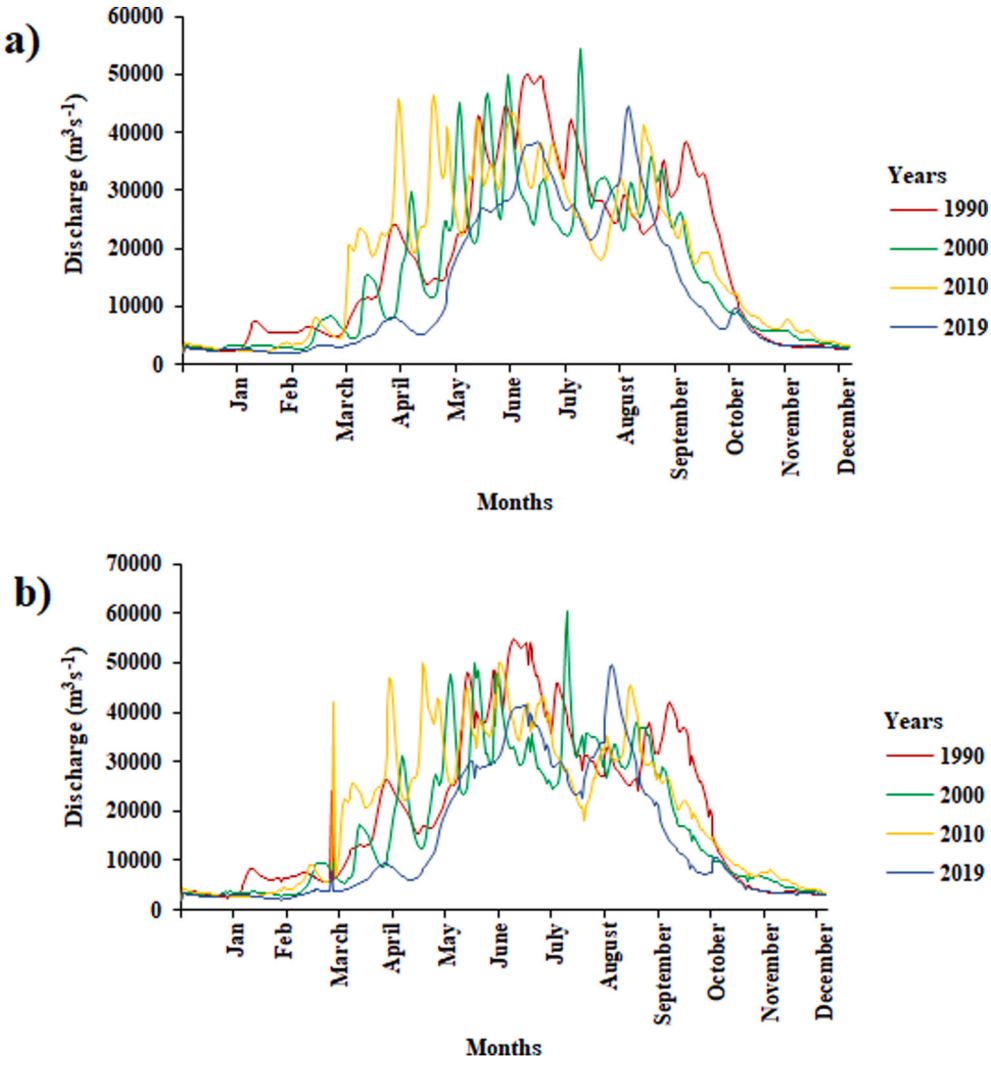

Fig. 5. Hydrograph of a) Silghat (Z3) b) Phulaguri (Z2) during 1990-2020.

for 396.24 km^2 which was more than erosion. Hence, the channel width and braiding increased.

The results of the study revealed that channel stability was primarily influenced by channel activity, average channel width and braiding. The contribution of these parameters was significant across all zones. The high rates of erosion-accretion implied the occurrence of a high level of channel activity. Deposition was observed to be more than erosion in all zones in the study duration. This showed that the sediment load was considerably high in the channel. Also, the gradient of the river channel was very low ranging from 0.4 m/km to 0.1 m/km. This further reduced the stream velocity. With such low stream power, sediment deposition increased and channel widening and braiding became more prominent which escalated the risks of bank erosion. Furthermore, a high discharge rate caused irregularities in bedload which led to the creation of a wider channel and braided pattern (Montgomery and Buffington, 1998; Sarma and Acharjee, 2018; Wolman and Brush, 1961). The discharge rates of two stations Phulaguri, located in Z2 (highly unstable) and Silghat, situated in Z3 (most stable) were analyzed (Fig. 5). Discharge stations were not situated in the other three zones. The hydrograph of Silghat showed peak discharges from June to October. The highest discharge of 54,413.72 m^3/s^{-1} was registered on August 6, 2000 and the average discharge during 1990-2020 was estimated at 16,176.65 m^3/s^{-1}. Similarly, the hydrograph of Phulaguri revealed peak discharges during the monsoonal months from June to October. The highest discharge of 60, 647.28 m^3/s^{-1} was recorded on August 6, 2000 and the average discharge rate was 18,041.01 m^3/s^{-1} during 1990-2020. The readings of Z2 were relatively higher compared to the readings in Z3. The means of channel width and BI of Z2 were also higher than Z3 during the study period. Thus, a higher discharge rate could lead to a wider channel and a high level of braiding. It was also noticed that sinuosity had a lesser impact on channel instability compared to the other parameters. Low SSI was registered for all zones and the values did not show high fluctuations. The river was sinuous and did not display meandering in any zone throughout the duration of the study.

All zones except Z3 have been identified as priority zones since these zones have exhibited considerable channel instability. The areas along these stretches face the risk of channel migration and bank failure. A study by Bhuyan et al. (2023) showed that the bank lines along the Middle Brahmaputra channel have migrated and faced severe bank avulsion. The study has also predicted further bank line changes which pose a threat to the population and ecology of the floodplains. The present study also found that the Middle Brahmaputra River is an unstable channel with very high discharge rates and crucial amounts of sediment. This makes it essential to minimise the unstable nature of the river. Sediment management could be carried out through sediment traps wherein the bed of the river is dug out and the sediments are confined in the created depression (Kumar, 2022). Dredging is proposed for removing sediment by digging out silt from the riverbed (Water Resources). This would regulate the sediment capacity of the channel and lessen the risk of bank erosion. Other measures to reduce instability and bank erosion include the cultivation of mixed tree species like *Bombax ceiba*, *Gmelina arborea*, *Samanea saman*, *Dalbergia sissoo* and *Tetrameles nudiflora* and indigenous species like bamboo (Gogoi et al., 2021; Guha, 2021). Afforestation in the upstream reaches and landslide-prone areas must be practiced to reduce landslide risks and regulate sediment generation. The construction of embankments and porcupines would help ensure more resilient banks (Bhuyan et al., 2024; Saikia and Mahanta, 2023). The use of geobags could also reduce the rate of bank erosion and further flow of sediments into the channel (Maurya et al., 2022; Thompson et al., 2020).

6. Conclusion

The Middle Brahmaputra River demonstrated dynamic attributes with varying degree of channel stability during 1990-2020. Channel stability was assessed through a channel stability index constructed using the parameters of channel activity, average channel width, braiding index and standard sinuosity index. Z3 was identified as the most stable channel whereas Z4 and Z5 were moderately stable. The most unstable reaches of the channel were Z1 and Z2. Thus, Z1, Z2, Z4 and Z5 were recognized as the priority zones that require immediate attention for river and erosion management strategies. The parameters of average channel width, braiding and channel activity primarily impacted channel stability. The river was highly braided throughout its course. The river was also found to be sinuous but not meandering and in certain zones, specifically Z3, the river almost assumed a straight path. Channel sinuosity was impacted by both topography and hydraulic controls, however, the influence of topography was comparatively greater. The presence of easily erodible silty and sandy soils, high discharge, high sediment load and low gradient which reduced stream power aided channel instability and bank erosion. Sediment traps, dredging, afforestation, the use of geotextile engineering and the construction of embankments and porcupines could be used to control sediment generation and bank erosion. The Middle Brahmaputra River exhibited an erratic and unstable behaviour and therefore, it is necessary to formulate plans and policies vested in the sustainable management of this vital watercourse. The study, however, has certain limitations. The analysis primarily relied on moderate-resolution satellite imagery which may have constrained the accurate detection and delineation of fine-scale spatial details. The lack of high-resolution satellite imagery for earlier decades also hindered the extension of the study period, thereby, narrowing the possibility of longer temporal trends. Furthermore, the availability and accessibility of long-term hydrological data was limited. This potentially restricted a more comprehensive fluvial dynamics assessment. Future research could address these limitations through the integration of higher-resolution remote sensing datasets and improved access to hydrological records. Moreover, studies could also combine hydrological parameters with topographical and geotechnical factors for a holistic channel dynamics study. Nevertheless, the methodology adopted by this study has a global appeal since it could be utilized to assess channel stability across diverse geographical units.

Author agreement statement

We the undersigned declare that this manuscript is original, has not been published before and is not currently being considered for publication elsewhere.

We confirm that the manuscript has been read and approved by all named authors and that there are no other persons who satisfied the criteria for authorship but are not listed. We further confirm that the order of authors listed in the manuscript has been approved by all of us.

We understand that the Corresponding Author is the sole contact for the Editorial process. He/she is responsible for communicating with the other authors about progress, submissions of revisions and final approval of proofs.

Funding

This research did not receive any specific grant from funding agencies in the public, commercial, or not-for-profit sectors.

CRediT authorship contribution statement

Nirsobha Bhuyan: Conceptualization, Data curation, Formal analysis, Investigation, Methodology, Software, Writing – original draft, Writing – review & editing. **Haroon Sajjad:** Supervision, Writing – review & editing. **Aastha Sharma:** Data curation, Writing – original draft. **Yatendra Sharma:** Data curation. **Raihan Ahmed:** Methodology.

Declaration of competing interest

The authors declare that they have no known competing financial

interests or personal relationships that could have appeared to influence the work reported in this paper.

Acknowledgement

The authors express deep gratitude to Water Resources, Government of Assam, India for the provision of hydrological data. We are extremely thankful to the anonymous reviewer for their valuable time in evaluating our manuscript and making constructive comments and suggestions.

Data availability

The authors confirm that all data generated or analyzed during this study are included in this article.

References

Acharjee, S., et al., 2022. Channel Migration and Consequential Land Use Land Cover Changes of Subansiri River, Assam, North-Eastern India. IOP Conf. Ser.: Earth Environ. Sci. 1032, 012009. https://doi.org/10.1088/1755-1315/1032/1/012009.

Ahammed, K.K.B., Pandey, A.C., 2019. Shoreline morphology changes along the Eastern Coast of India, Andhra Pradesh by using geo spatial technology. J. Coast Conserv. 23, 331–353. https://doi.org/10.1007/s11852-018-0662-5.

Ahmed, I., et al., 2018. Erosion induced channel migration and its impact on dwellers in the Lower Gumti River, Tripura, India. Spat. Inf. Res. 26, 537–549. https://doi.org/10.1007/s41324-018-0196-9.

Akhtar, M.P., et al., 2011. Braiding process and bank erosion in the Brahmaputra River. Int. J. Sediment Res. 26, 431–444. https://doi.org/10.1016/S1001-6279(12)60003-1.

Bhattacharya, R.K., et al., 2022. Channel instability and hydrogeomorphic adjustment in alluvial reach of Kangsabati River, India using digital shoreline analysis system and acoustic doppler current profiler. Geocarto Int. 37, 16232–16260. https://doi.org/10.1080/10106049.2022.2107712.

Bhuyan, N., et al., 2023. Estimating bank-line migration of the Brahmaputra river in the Middle Brahmaputra floodplains of Assam, India using digital shoreline analysis system. Environ. Earth Sci. 82, 385. https://doi.org/10.1007/s12665-023-11061-4.

Bhuyan, N., et al., 2024. Assessing landscape ecological vulnerability to riverbank erosion in the Middle Brahmaputra floodplains of Assam, India using machine learning algorithms. Catena 234, 107581. https://doi.org/10.1016/j.catena.2023.107581.

Biswas, R., Anwaruzzaman, A.K., 2019. Measuring hazard vulnerability by bank erosion of the Ganga River in Malda district using PAR model. J. Geogr. Environ. Earth Sci. Int. 22, 1–15. https://doi.org/10.9734/JGEESI/2019/v22i130136.

Census of India, 2011. Office of the registrar general and census commissioner. India. URL. https://censusindia.gov.in/census.website/data/population-finder. (Accessed 27 May 2023).

Chakraborty, K., Saha, S., 2022. Assessment of bank erosion and its impact on land use and land cover dynamics of Mahananda River basin (Upper) in the Sub-Himalayan North Bengal, India. SN Appl. Sci. 4, 20. https://doi.org/10.1007/s42452-021-04904-x.

Das, T.K., et al., 2014. River bank erosion induced human displacement and its consequences. Living Rev. Landsc. Res. 8, 3. https://doi.org/10.12942/lrlr-2014-3.

Das, V.K., et al., 2020. Cohesive river bank erosion mechanism under wave-current interaction: a flume study. J. Earth Syst. Sci. 129, 1–20. https://doi.org/10.1007/s12040-020-1363-7.

Das, R., Samanta, G., 2023. Impact of floods and river-bank erosion on the riverine people in Manikchak Block of Malda District, West Bengal. Environ. Dev. Sustain. 25, 13595–13617. https://doi.org/10.1007/s10668-022-02648-1.

Deb, M., Ferreira, C., 2015. Planform channel dynamics and bank migration hazard assessment of a highly sinuous river in the North-Eastern zone of Bangladesh. Environ. Earth Sci. 73, 6613–6623. https://doi.org/10.1007/s12665-014-3884-3.

Debnath, J., et al., 2017. Channel migration and its impact on land use/land cover using RS and GIS: a study on Khowai River of Tripura, North-East India. Egypt. J. Remote Sens. Space. Sci. 20, 197–210. https://doi.org/10.1016/j.ejrs.2017.01.009.

Debnath, J., et al., 2023. Shifting sands: assessing bankline shift using an automated approach in the JiaBharali River, India. Land 12, 703. https://doi.org/10.3390/land12030703.

Dey, S., Mandal, S., 2019. Assessing channel migration dynamics and vulnerability (1977–2018) of the Torsa River in the Duars and Tal region of eastern Himalayan foothills, West Bengal, India. Spat. Inf. Res. 27, 75–86. https://doi.org/10.1007/s41324-018-0213-z.

Endreny, T., 2006. Stream Stability Analysis. University at Buffalo. https://fgmorph.eng.buffalo.edu/fg_8_1.php. (Accessed 17 February 2024).

Fischenich, J.C., 1989. Channel erosion analysis and control. In: Woessmer, W., Potts, D. F. (Eds.), Symposium Proceedings of Headwaters Hydrology, American Water Resources Association, Bethesda, Md..

Ghosh, S., Mistri, B., 2012. Hydrogeomorphic significance of sinuosity index in relation to river instability: a case study of Damodar River, West Bengal, India. Int. J. Adv. Earth Sci. 1 (2), 49–57.

Ghosh, B., Mukhopadhyay, S., 2021. Channel planform dynamics, avulsion and bankline migration: a study in the monsoon-dominated Dwarkeswar river, Eastern India. Arabian J. Geosci. 14, 854. https://doi.org/10.1007/s12517-021-07270-5.

Ghosh, D., Sahu, A.S., 2019. Bank line migration and its impact on land use and land cover change: a case study in Jangipur subdivision of Murshidabad District, West Bengal. J. Indian Soc. Remote Sens. 47, 1969–1988. https://doi.org/10.1007/s12524-019-01043-0.

Gilfellon, G.B., et al., 2003. Channel and bed morphology of a part of the Brahmaputra River in Assam. J. Geol. Soc. India 62, 227–235.

Gogoi, A., et al., 2021. Plant biodiversity and carbon sequestration potential of the planted forest in Brahmaputra flood plains. J. Environ. Manag. 280, 111671. https://doi.org/10.1016/j.jenvman.2020.111671.

Gogoi, P., Sharma, N., 2021. Spatio-temporal study of morpho-dynamics of the Brahmaputra River along its Majuli Island reach. Environ. Chall., 100217 https://doi.org/10.1016/j.envc.2021.100217.

Guha, N., 2021. Planted Forests can Tackle Flood and Erosion Impacts along the Brahmaputra. Mongabay. https://india.mongabay.com/2021/11/planted-forests-can-tackle-flood-and-erosion-impacts-along-the-brahmaputra/. (Accessed 27 May 2023).

Haron, N.A., et al., 2022. Morphological assessment of river stability: review of the most influential parameters. Sustainability 14, 10025. https://doi.org/10.3390/su141610025.

Hazarika, N., et al., 2015. Assessing land-use changes driven by river dynamics in chronically flood affected Upper Brahmaputra plains, India, using RS- GIS techniques. Egypt. J. Remote Sens. Sp. Sci. 18, 107–118. https://doi.org/10.1016/j.ejrs.2015.02.001.

Hekal, N., 2018. Evaluation of the equilibrium of the River Nile morphological changes throughout “Assuit-Delta Barrages” reach. Water Sci. 32, 230–240.

Hosu, M., Sabo, H., 2012. The morphodynamics of the somes river channel, Northwestern Romania, as response to natural influences. APCBEE Proc. 1, 210–215.

Jodhani, K.H., et al., 2024. Channel planform dynamics using earth observations across Rel River, Western India: a synergetic approach. Spat. Inf. Res. https://doi.org/10.1007/s41324-024-00573-1.

Khan, M.H., 2012. River erosion and its socio-economic impact in Barpeta district with special reference to Mandia development block of Assam. Int. J. Eng. Sci. 1, 177–183.

Khan, A., et al., 2018. Characterization of channel planform features and sinuosity indices in parts of Yamuna River flood plain using remote sensing and GIS techniques. Arabian J. Geosci. 11, 525. https://doi.org/10.1007/s12517-018-3876-9.

Konsoer, K.M., et al., 2016. Spatial variability in bank resistance to erosion on a large meandering, mixed bedrock-alluvial river. Geomorphology 252, 80–97. https://doi.org/10.1016/j.geomorph.2015.08.002.

Kotoky, P., et al., 2015. Spatio-temporal variations of erosion-deposition in the Brahmaputra river, Majuli-Kaziranga sector, Assam: implications on flood management and flow mitigation. In: Ramkumar, M., Kumaraswamy, K., Mohanraj, R. (Eds.), Environmental Management of River Basin Ecosystems. Springer Earth System Sciences, pp. 227–251. https://doi.org/10.1007/9783-319-13425-3_12.

Kumar, A., 2022. Sediment Management for the Brahmaputra River. Maritime Research Center. https://mrc.foundationforuda.in/sediment-management-for-the-brahmaputra-river/#:~:text=Erosion%20management%20measures%20are%20implemented,slowing%20the%20rate%20of%20sedimentation. (Accessed 8 April 2024).

Kumar, K.S.A., et al., 2020. Geology and geomorphology. In: Mishra, B.B. (Ed.), The Soils of India. Springer International Publishing, Berlin, pp. 57–79. https://doi.org/10.1007/978-3-030-31082-0_4.

Kuo, C.-W., et al., 2017. Channel planform dynamics monitoring and channel stability assessment in two sediment-rich rivers in Taiwan. Water 9, 84. https://doi.org/10.3390/w9020084.

Leopold, L.B., et al., 1964. Fluvial Processes in Geomorphology. Freeman, San Francisco, Calif., p. 522

Leopold, L.B., Wolman, M.G., 1957. River channel patterns, braided, meandering and straight. U. S. Geol. Surv. Prof. Pap. 282-B, 39–85.

Mandarino, A., et al., 2019. Channel planform changes along the Scrivia River floodplain reach in northwest Italy from 1878 to 2016. Quat. Res. 91, 620–637. https://doi.org/10.1017/qua.2018.67.

Maurya, S., et al., 2022. Use of geosynthetics as a soft structural measure to mitigate flood hazard and bank erosion problem. In: Reddy, C.N.V.S., Saride, S., Krishna, A.M. (Eds.), Ground Improvement and Reinforced Soil Structures, Lecture Notes in Civil Engineering. Springer, Singapore, pp. 751–763. https://doi.org/10.1007/978-981-16-1831-4_67.

McMahon, W.J., Davies, N.S., 2018. The shortage of geological evidence for pre-vegetation meandering rivers. Int. Assoc. Sedimentol. Spec. Publ. 48, 119–148. https://doi.org/10.1002/9781119424437.ch5.

Mehtani, P., 2017. Channel Morphology. E-Pathshala. https://epgp.inflibnet.ac.in/epgpdata/uploads/epgp_content/S000017GE/P001786/M025390/ET/1512629888Channel_Morphology-Final(1.pdf. (Accessed 8 May 2024).

Montgomery, D.R., Buffington, J.M., 1998. Channel processes, classification, and response. In: Naiman, R.J., Bilby, R.E. (Eds.), River Ecology and Management: Lessons from the Pacific Coastal Ecoregion. Springer-Verlag, New York, NY, pp. 13–42.

Mueller, J.E., 1968. An introduction to the hydraulic and topographic sinuosity indexes. Ann. Assoc. Am. Geogr. 58 (2), 371–385.

Nath, A., Ghosh, S., 2022. Meandering rivers' morphological changes analysis and prediction – a case study of Barak river, Assam. H_2Open J. 5 (2), 289. https://doi.org/10.2166/h2oj.2022.003.

Nath, M.J., Medhi, H., 2021. River bank line shift caused by Brahmaputra in Morigaon District, Assam (1996–2021). Int. J. Lakes Rivers (IJLR) 14, 237–249.
Nelson, N.C., et al., 2013. Spatial and temporal patterns in channel change on the Snake River downstream from Jackson lake dam, Wyoming. Geomorphology 200, 132–142.
Northwest Hydraulics Consultants, 2006. River Flooding and Erosion in Northeast India. Background Paper No. 4.
Rajmohan, N., Prathapar, S.A., 2013. Hydrogeology of the Eastern Ganges Basin: an Overview. International Water Management Institute (IWMI). https://doi.org/10.5337/2013.216.
Rakovan, M.T., Renwick, W.H., 2011. The role of sediment supply in channel instability and stream restoration. J. Soil Water Conserv. 66, 40–50. https://doi.org/10.2489/jswc.66.1.40.
Ratzlaff, J., 1991. Sinuosity components of the upper Saline River Valley, Western Kansas. Trans. Kans. Acad. Sci. 94, 46–57. https://doi.org/10.2307/3628040.
Sah, R.K., Das, A.K., 2018. Morphological dynamics of the Rivers of Brahmaputra. J. Geol. Soc. India 92, 441–448. https://doi.org/10.1007/s12594-018-1039-y.
Sahay, A., et al., 2020. Understanding riverbank erosion in Majuli Island of India: geomorphological process and policy implications. Focus Geogr. 1–2. https://doi.org/10.21690/foge/2020.63.7f.
Saikia, L., et al., 2019. Erosion–deposition and land use/land cover of the Brahmaputra River in Assam, India. J. Earth Syst. Sci. 128, 1–12. https://doi.org/10.1007/s12040-019-1233-3.
Saikia, M., Mahanta, R., 2023. Riverbank erosion and vulnerability – a study on the char dwellers of Assam, India. Nat. Hazards Res. 4, 274–287. https://doi.org/10.1016/j.nhres.2023.10.007.
Sarkar, A., et al., 2012. RS-GIS based assessment of river dynamics of Brahmaputra River in India. J.Water Resour. Prot. 38, 26–39. https://doi.org/10.4236/jwarp.2012.42008.
Sarma, J.N., et al., 2007. Change of river channel and bank erosion of the Burhidihing River (Assam), assessed using remote sensing data and GIS. J. Indian Soc. Remote Sens. 35, 93–100. https://doi.org/10.1007/BF02991837.
Sarma, J.N., Acharjee, S.A., 2018. Study on variation in channel width and braiding intensity of the Brahmaputra River in Assam, India. Geosciences 8, 343. https://doi.org/10.3390/geosciences8090343.
Sarma, J.N., Phukan, M.K., 2006. Bank erosion and bankline migration of the Brahmaputra River in Assam during the twentieth century. J. Geol. Soc. India 68, 1023–1036.
Schumm, S.A., 1961. Effect of Sediment Characteristics on Erosion and Deposition in Ephemeral-Stream Channels. Geol. Surv. Prof. Pap. 352-C. United States Government Printing Office, Washington.
Sharma, N., et al., 2010. Hazard, vulnerability and risk on the Brahmaputra basin: a case study of river bank erosion. Open Hydrol. J. 4, 211–226. https://doi.org/10.2174/1874378101004010211.
Siddha, S., Sahu, P., 2022. Impact of climate change on the river eco system. In: Madhav, S., Kanhaiya, S., Srivastav, A., Singh, V., Singh, P. (Eds.), Ecological Significance of River Ecosystems. Elsevier, Amsterdam, pp. 79–104.
Simon, A., et al., 2000. Bank and near-bank processes in an incised channel. Geomorphology 35, 193–217. https://doi.org/10.1016/S0169-555X(00)00036-2.
Soar, P.J., et al., 2017. Quantifying river channel stability at the basin scale. Water 9, 133. https://doi.org/10.3390/w9020133.
Suresh, A., et al., 2022. A geospatial approach in modelling the morphometric characteristics and course of Brahmaputra river using sinuosity index. Environ. Sustain. Indic. 15, 100196. https://doi.org/10.1016/j.indic.2022.100196.
Thomas, J., et al., 2019. Channel stability assessment in the lower reaches of the Krishna River (India) using multi-temporal satellite data during 1973–2015. Remote Sens. Appl.: Soc. Environ. 17. https://doi.org/10.1016/j.rsase.2019.100274.
Thompson, A., et al., 2020. Geobag stability for riverbank erosion protection structures: physical model study. Geotext. Geomembranes 48, 110–119. https://doi.org/10.1016/j.geotexmem.2019.103526.
Vazquez-Tarrio, D., et al., 2024. Effects of sediment transport on flood hazards: lessons learned and remaining challenges. Geomorphology 446, 108976. https://doi.org/10.1016/j.geomorph.2023.108976.
Water Resources. Flood and erosion problems. Gov. Assam. URL. https://waterresources.assam.gov.in/portlets/flood-erosion-problems. (Accessed 17 May 2024).
Wolman, M.G., Brush, L.M., 1961. Factors controlling the size and shape of stream channels in coarse noncohesive sands. U.S. Geological Survey Professional Paper 282, 28. https://doi.org/10.3133/pp282G.
Wu, T., et al., 2023. Channel activity remote sensing retrieval model: a case study of the Lower Yellow River. Remote Sens. 15, 3636. https://doi.org/10.3390/rs15143636.
Yang, J., et al., 2023. Numerical simulation of the composite bank stability process of the Songhua River. In: Li, Y., Hu, Y., Rigo, P., Lefler, F.E., Zhao, G. (Eds.), Proceedings of PIANC Smart Rivers 2022, PIANC 2022, Lecture Notes in Civil Engineering, 264. Springer, Singapore. https://doi.org/10.1007/978-981-19-6138-0_103.
Yousefi, S., et al., 2021. Geomorphological change detection of an urban meander loop caused by an extreme flood using remote sensing and bathymetry measurements (a case study of Karoon River, Iran). J. Hydrol. 597, 125712. https://doi.org/10.1016/j.jhydrol.2020.125712.
Yu, D., Xu, G., 2023. Analysis of river stability in the middle reaches of Huaihe River based on Non-equilibrium Thermodynamicsins. In: Li, Y., Hu, Y., Rigo, P., Lefler, F.E., Zhao, G. (Eds.), Proceedings of PIANC Smart Rivers 2022. PIANC 2022. Lecture Notes in Civil Engineering, 264. Springer, Singapore. https://doi.org/10.1007/978-981-19-6138-0_91.
Zesmill, 2016. River Instability. http://zesmill.com/watersheds-rivers-lakes/river-instability/. (Accessed 14 May 2024).
Zischg, A.P., 2023. Disentangling drivers of change. In: Zischg, A.P. (Ed.), Flood Risk Change. Elsevier, pp. 37–165. https://doi.org/10.1016/B978-0-12-822011-5.00006-5.